

## **ACCURACY AND COMPLEXITY ASSESSMENT OF SUB-DOMAIN MOMENT METHODS FOR ARRAYS OF THIN-WIRE LOOPS**

**P. J. Papakanellos**

School of Electrical and Computer Engineering  
National Technical University of Athens  
GR 157-73 Zografou, Athens, Greece

**Abstract**—A direct sub-domain moment-method formulation is presented for the analysis of arrays of thin-wire loops. Curved piecewise sinusoidal basis functions are used for the description of the currents on the loops, while both point matching and reaction matching are examined as testing schemes. Numerical results are provided for representative array structures with the intention to delve into the behavior of the solutions as the number of basis/testing functions grows, but also for the purpose of comparison with well-documented results. Finally, the complexity of the developed codes is estimated and general guidelines are provided for the efficient and accurate analysis of multi-element arrays.

### **1. INTRODUCTION**

Traditionally, isolated thin-wire loop antennas have been analyzed with the aid of Fourier expansions. In this approach, the unknown current on the loop, the kernel of the associated integral equation and the driving field are expressed as Fourier series, the coefficients of which can be readily interrelated. The resulting current coefficients are available in closed form for different excitation types; for example, see [1–5] and certain works cited therein. The suitability of Fourier series for the description of the currents on thin-wire loops has led to the generalization of their use to coupled loops and arrays of loop elements [6–10]. Nevertheless, the applicability of this approach is practically restricted to specific array configurations, while the computation of the resulting expansion coefficients via numerical integration becomes increasingly problematic as the loop circumference is increased, as an outcome of the fact that more and more terms are required to obtain

fairly stable results. As an alternative, one can utilize moment methods [11], which have been developed in several variants for treating curved thin-wire structures (see, for example, [12, 13]).

Moment methods may be applied to thin-wire loops using either entire-domain or sub-domain basis and testing functions. Entire-domain schemes are available for both isolated loops [14] and arrays of arbitrarily oriented loops [15]. However, entire-domain schemes are applicable under restrictions upon the size of the loop, mainly due to certain difficulties encountered when attempting to calculate the associated integrals for large mode numbers. On the other hand, sub-domain schemes are relatively easy to implement, even for quite large loops [16–18].

The present article is an outgrowth of the work presented in [18]. More specifically, the sub-domain moment-method formulation of [18] is extended to cope with arrays of arbitrarily large loops. As in [18], both a simple collocation scheme and Galerkin’s method are adopted as testing procedures. The two variants of the proposed method are examined from different aspects, with special emphasis placed on the behavior of the resulting solutions as the number of basis/testing functions grows. For the assessment of the computational complexity of the developed codes, cost functions are estimated in the form of simple polynomial expressions, which are further utilized to obtain rough quantitative criteria for the efficient utilization of these codes.

For the purpose of comparison with well-documented results [6], numerical results are presented for a pair of parallel identical loops. Results are also presented for multi-element arrays of parallel loops, in order to verify the findings of the complexity analysis and demonstrate the important savings in execution times that can be achieved by applying Galerkin’s method for relatively small numbers of unknowns.

## 2. MOMENT-METHOD FORMULATION FOR ARRAYS OF THIN-WIRE LOOPS

Consider an array of  $L$  thin-wire loops, each of which may be either active (that is, directly driven by a generator) or parasitic. The radius of each loop and the corresponding wire radius are denoted by  $b_p$  and  $a_p$ , respectively. The respective loop center is at  $(x_p, y_p, z_p)$  in rectangular coordinates. The subscript  $p = 1, 2, \dots, L$  is used to distinguish among the quantities pertaining to each element of the array. The loops are thin in the sense that  $a_p \ll b_p$  and  $a_p \ll \lambda$ , where  $\lambda$  is the operating wavelength; hence, the unknown currents on the loops can be assumed to flow predominantly in the respective longitudinal directions. Frill sources of equivalent voltages  $V_p$  are assumed for the

excitation of the active array elements; nevertheless, the analysis that follows can be easily adapted to other excitation models.

Since the main scope of the present study is the examination of the proposed numerical schemes from different aspects, including that of computational accuracy and complexity, it is rather convenient to focus on arrays of loops that are parallel to each other. For this, the array elements are all lying in parallel planes specified by  $z = z_p$ . The generalization of the proposed formulation to arrays of arbitrarily oriented loops requires rather formidable algebraic manipulations [15] and is beyond the scope of this article.

The unknown longitudinal current on each element of the array is approximated by a weighted superposition of  $2N_p$  sub-domain basis functions and can be expressed as a function of the local azimuth angle  $\xi$  around the respective periphery, as follows

$$I_p(\xi) = \sum_{n=1}^{2N_p} w_{(p,n)} f_{(p,n)}(\xi), \quad (1)$$

where  $w_{(p,n)}$  are unknown weights. The basis functions  $f_{(p,n)}(\xi)$  are selected to be piecewise sinusoids of curvature radius  $b_p$  and angular width  $2\delta_p = 2\pi/N_p$ , which are centered at  $(n-1)\delta_p$  and can be written as

$$f_{(p,n)}(\xi) = \begin{cases} \sin\{k_0 b_p [\delta_p - |\xi - (n-1)\delta_p|]\}, & |\xi - (n-1)\delta_p| \leq \delta_p \\ 0, & |\xi - (n-1)\delta_p| > \delta_p \end{cases} \quad n = 1, 2, \dots, 2N_p, \quad (2)$$

where  $k_0 = 2\pi/\lambda$ . The subscript pair  $(p, n)$  is introduced to distinguish among quantities pertaining to the basis functions of (2). For example, the vector  $\vec{E}_{(p,n)}$  that appears below stands for the electric field radiated by the current of (2).

Instead of determining coupled integral equations for the unknown currents on the array elements, the boundary condition of the tangential electric field around the periphery of each element is enforced in a direct manner, as in [18]. This is accomplished by simply equating the tangential component of the total electric field radiated by the filamentary currents of (1) to the negative of the corresponding component of the excitation field on each element. For reasons explained in [18], the contribution of the self-excited electric field to the tangential electric field on each loop is evaluated along a testing ring defined by the upper (or lower) points of the associated wire. On the other hand, as long as sufficiently thin loops are considered, mutual-coupling effects are taken into account in an average sense;

in particular, by computing the tangential electric field generated by the distant basis functions along the wire axis. Hence, the boundary conditions on the array elements can be written as

$$\begin{aligned} & \sum_{n=1}^{2N_q} w_{(q,n)} \left[ \hat{t}_q \cdot \vec{E}_{(q,n)}(x_q + b_q \cos \xi, y_q + b_q \sin \xi, z_q + a_q) \right] \\ & + \sum_{\substack{p=1 \\ p \neq q}}^L \sum_{n=1}^{2N_p} w_{(p,n)} \left[ \hat{t}_q \cdot \vec{E}_{(p,n)}(x_q + b_q \cos \xi, y_q + b_q \sin \xi, z_q) \right] \\ & = -\hat{t}_q \cdot \vec{E}_q^{\text{exc}}(x_q + b_q \cos \xi, y_q + b_q \sin \xi, z_q + a_q), \quad q = 1, 2, \dots, L, \end{aligned} \quad (3)$$

where  $\xi$  is the local azimuth angle as measured around the testing ring along which the boundary condition is enforced and  $\hat{t}_q = -\hat{x} \sin \xi + \hat{y} \cos \xi$  is the associated tangential unit vector. The excitation fields of the active elements are denoted by  $\vec{E}_q^{\text{exc}}$  in (3). Parasitic elements are simply modeled as active elements driven by null fields. Explicit expressions for the electric fields of the basis functions can be derived by properly shifting the near-field components given in the Appendix of [18].

Next, the boundary conditions of (3) are utilized in two different ways, in order to form systems of linear equations for the unknown coefficients  $w_{(p,n)}$ . A simple way to proceed is to apply a simple point-matching (PM) procedure, according to which (3) is enforced at a mesh of discrete points, which is accomplished by setting  $\xi \rightarrow (m-1)\delta_q$  for  $m = 1, 2, \dots, 2N_q$ . Alternatively, one can apply Galerkin's method and enforce (3) in a reaction-matching (RM) fashion; this essentially consists in multiplying both sides of (3) by the testing functions  $f_{(q,m)}(\xi)$  and integrating over the intervals spanned by these functions. In this latter case, the resulting simultaneous equations may be written as

$$\sum_{p=1}^L \sum_{n=1}^{2N_p} Z_{(p,n),(q,m)} w_{(p,n)} = -V_{(q,m)}, \quad q = 1, 2, \dots, L, \quad m = 1, 2, \dots, 2N_q. \quad (4)$$

The reaction integrals  $Z_{(p,n),(q,m)}$  and the excitation terms  $V_{(q,m)}$  are given by

$$Z_{(p,n),(q,m)} = - \int_{(m-2)\delta_q}^{m\delta_q} S_{(p,n),q}(\xi) f_{(q,m)}(\xi) b d\xi, \quad (5)$$

$$V_{(q,m)} = - \int_{(m-2)\delta_q}^{m\delta_q} S_q^{\text{exc}}(\xi) f_{(q,m)}(\xi) b d\xi, \quad (6)$$

where  $S_{(p,n),q}(\xi)$  and  $S_q^{\text{exc}}(\xi)$  are the following inner products

$$S_{(p,n),q}(\xi) = \begin{cases} \hat{t}_q \cdot \vec{E}_{(p,n)}(x_q + b_q \cos \xi, y_q + b_q \sin \xi, z_q + a_q), & p = q \\ \hat{t}_q \cdot \vec{E}_{(p,n)}(x_q + b_q \cos \xi, y_q + b_q \sin \xi, z_q), & p \neq q \end{cases}, \quad (7)$$

$$S_q^{\text{exc}}(\xi) = \hat{t}_q \cdot \vec{E}_q^{\text{exc}}(x_q + b_q \cos \xi, y_q + b_q \sin \xi, z_q + a_q). \quad (8)$$

Rigorous expressions for the excitation field of the frill generator are available in [5]. To simplify the relevant computations, the approximations suggested and exploited in [17] are utilized, which yield

$$S_q^{\text{exc}}(\xi) \approx -\frac{V_q \cos \xi}{\ln\left(\frac{c_q}{a_q}\right)} \left[ \frac{\exp\left(-jk_0 \sqrt{c_q^2 + 4b_q^2 \sin^2 \frac{\xi}{2}}\right)}{\sqrt{c_q^2 + 4b_q^2 \sin^2 \frac{\xi}{2}}} - \frac{\exp\left(-jk_0 \sqrt{a_q^2 + 4b_q^2 \sin^2 \frac{\xi}{2}}\right)}{\sqrt{a_q^2 + 4b_q^2 \sin^2 \frac{\xi}{2}}} \right] \quad (9)$$

where  $c_q/a_q$  is the ratio of the outer to the inner radius of the equivalent frill current. The above formulation can be readily adapted to other excitation models; for the rather popular delta-gap source, the resulting expressions can be found in [18]. When combined with non-singular kernels, this latter feeding model yields nonphysical currents whose imaginary part oscillates rapidly near the driving point [18]. Because of this fact, the delta-gap excitation is not considered further herein.

As can be readily deduced, the computation of the reaction integrals  $Z_{(p,n),(q,m)}$  is quite cumbersome. Important savings in the computation of the self-reaction integrals (occurring for  $p = q$ ) can be achieved by utilizing the symmetry properties of each element, yielding  $Z_{(p,n),(p,m)} = Z_{(p,1),(p,|n-m|+1)}$ . Furthermore, when any two loops are more distant than a few wire radii, which is the case usually encountered in practice, the associated reaction integrals  $Z_{(p,n),(q,m)}$  between segments belonging to different loops can be readily computed using elementary quadrature techniques, like the two-term midpoint rule

$$Z_{(p,n),(q,m)} \approx -b\delta_q \left[ S_{(p,n),q}(m\delta_q - 1.5\delta_q) f_{(q,m)}(m\delta_q - 1.5\delta_q) \right]$$

$$+ S_{(p,n),q}(m\delta_q - 0.5\delta_q)f_{(q,m)}(m\delta_q - 0.5\delta_q)] \quad (10)$$

Similar formulas can be also used for the computation of the integrals  $V_{(q,m)}$  that correspond to integration intervals quite far from the feeding points and the reaction integrals  $Z_{(p,n),(p,m)}$  between sufficiently distant segments belonging to the same loop. The midpoint formula for  $V_{(q,m)}$  can be written as

$$V_{(q,m)} \approx -b\delta_q \left[ S_q^{\text{exc}}(m\delta_q - 1.5\delta_q)f_{(q,m)}(m\delta_q - 1.5\delta_q) + S_q^{\text{exc}}(m\delta_q - 0.5\delta_q)f_{(q,m)}(m\delta_q - 0.5\delta_q) \right] \quad (11)$$

Several tests have shown that the efficient midpoint formulas (10) and (11) can be used for the computation of interactions that are more distant than a properly selected threshold, without any perceivable loss of accuracy. In most cases, a distance threshold level at  $25a_q$  was found to be a good choice.

### 3. VALIDATION RESULTS

Certain tests have been conducted for the verification of the numerical schemes presented in this article. Much care was taken to ensure the accuracy of the computations, especially in view of the rapidly growing condition numbers that typically accompany thin-wire moment-method formulations with non-singular kernels. For this, quadrature rules of varying order and different system solvers were implemented.

As a first example, the case of two parallel identical loops is examined. In what follows, the distance between their centers is denoted by  $d$ . Numerical results for the self- ( $Y_{1,1} = G_{1,1} + jB_{1,1}$ ) and mutual ( $Y_{1,2} = G_{1,2} + jB_{1,2}$ ) admittance as  $N$  (where  $N_1 = N_2 = N$ ) grows are presented in Figs. 1 and 2, respectively, for  $k_0b = 1$ ,  $\Omega = 2\ln(2\pi b/a) = 10$ ,  $c/a = 2.3$  and  $k_0d = 2$ . The solid lines in Figs. 1 and 2 show independent results taken from [6]. Apparently, when  $N$  is sufficiently large, the agreement between the results of the proposed schemes and the reference ones is excellent. The PM and RM points become graphically indistinguishable as  $N$  increases up to 75 (note that  $\pi b/a \approx 74.23$  in this example), just as expected according to [18]. On the contrary, glaring differences between the PM and RM results are seen for small  $N$ . Obviously, the RM results are remarkably stable over the whole range of  $N$  (even for  $N$  as small as 5), while the PM results exhibit a strong dependence upon  $N$ , especially when  $N$  is moderately small; note that certain points of the PM data set are out of scale in Figs. 1 and 2. This behavior is representative over a wide range of loop lengths and radii, at least for sufficiently thin wires.

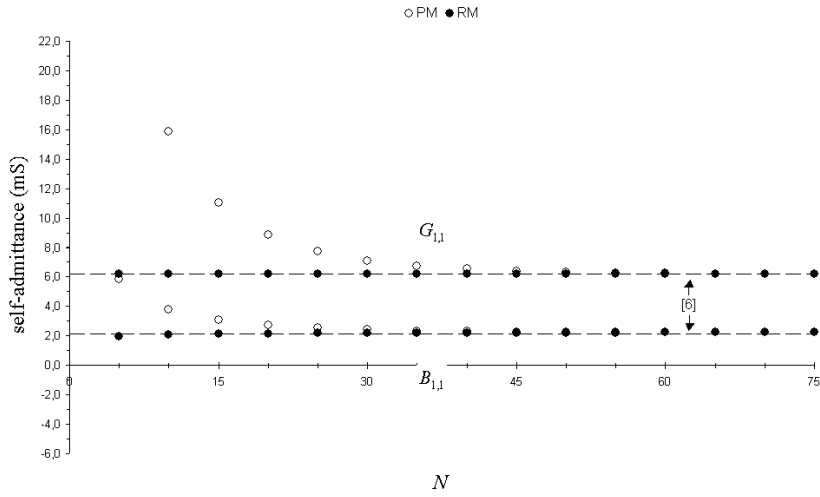


**Figure 1.** Computed results for the self-admittance of two parallel identical loops as  $N$  grows, for  $k_0b = 1$ ,  $\Omega = 2 \ln(2\pi b/a) = 10$ ,  $c/a = 2.3$  and  $k_0d = 2$ .

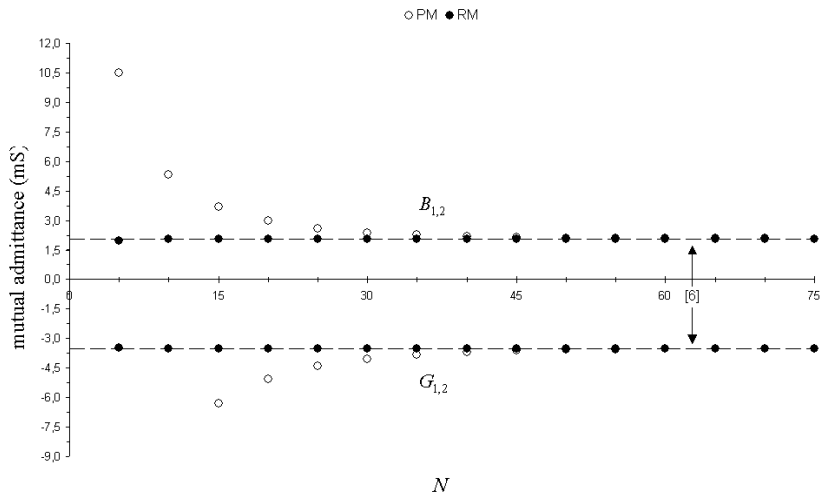


**Figure 2.** Computed results for the mutual admittance of two parallel identical loops as  $N$  grows, for  $k_0b = 1$ ,  $\Omega = 2 \ln(2\pi b/a) = 10$ ,  $c/a = 2.3$  and  $k_0d = 2$ .

To further investigate the behavior of the solutions, selected results are presented in Figs. 3 (PM) and 4 (RM) for the self- and mutual admittances as functions of  $d/\lambda$ . The plotted results are for  $k_0b = 1$ ,  $\Omega = 2 \ln(2\pi b/a) = 10$  and  $c/a = 2.3$ . Numerous runs have been performed for different discretization levels, ranging from high ( $N$  roughly equal to or larger than  $\pi b/a$ ) to low ( $N$  much smaller than  $\pi b/a$ ), in order to verify the findings of the previous paragraph; for brevity, results for  $N = 75$  and  $N = 25$  are shown in Figs. 3 and 4. Just as expected from the preceding, the RM curves in Fig. 4 are in very close agreement to each other, while significant discrepancies exist between the PM curves in Fig. 3.

Several other configurations were examined, in order to look into the capabilities of the proposed schemes for analyzing multi-element arrays. Among others, many of the Yagi arrays tabulated in [19] were analyzed and certain of the characteristics reported therein were adequately reproduced (within about 1%).

#### 4. COMPUTATIONAL COST ESTIMATION

As pointed out in [18], the simplicity of the PM scheme cannot guarantee its unconditional superiority over the RM one in terms of typical efficiency measures, since the latter yields stable solutions for notably smaller numbers of unknowns. This feature of the RM scheme is particularly useful when one is interested in analyzing large-scale arrays or in performing repeated simulations as part of an optimization process. The purpose of this section is to provide cost functions for the developed codes, mainly in order to carry out complexity comparisons on a systematic basis (in the sense discussed in [20]) and examine the potential savings that may be achieved by applying the RM scheme for relatively small numbers of basis functions per element.

As can be easily deduced, the application of sub-domain moment methods to multi-element arrays of loops leads to large interaction matrices that are not symmetric Toeplitz ones, even when the loops are parallel to each other and arranged in a row. As an outcome, by contrast with what is true for single loops, fast solvers intended for Toeplitz matrices are not applicable and the associated linear systems must be solved via general-purpose algorithms. To simplify the analysis that follows, only arrays of coaxial loops are considered, which have been used in a multitude of practical applications. The general case of  $L$  driven loops is assumed, in order to take into account the maximum number of complex operations that may be required for the computation of nonzero excitation terms  $V_{(q,m)}$ .

For a  $G$ -point Gauss-Legendre quadrature routine and a complex

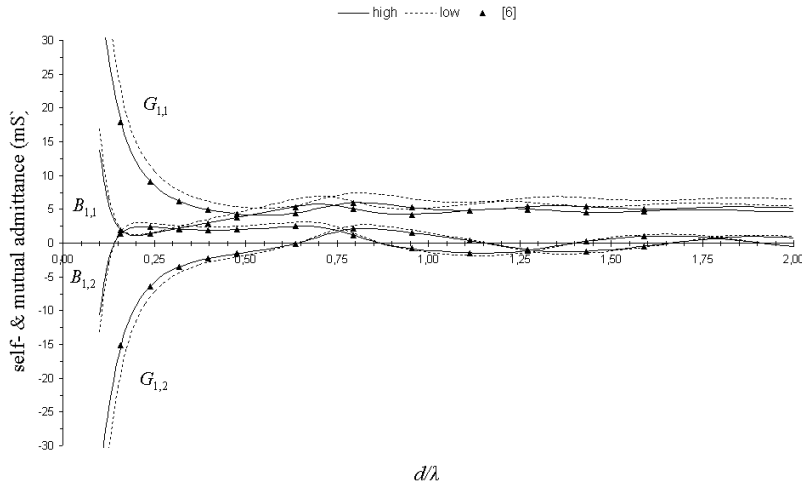


**Figure 3.** Plot of the self- and mutual admittances of two parallel identical loops as functions of  $d/\lambda$ , as derived by the PM scheme, for  $k_0b = 1$ ,  $\Omega = 2 \ln(2\pi b/a) = 10$  and  $c/a = 2.3$ . High and low discretization levels correspond to  $N = 75$  and  $N = 25$ , respectively.

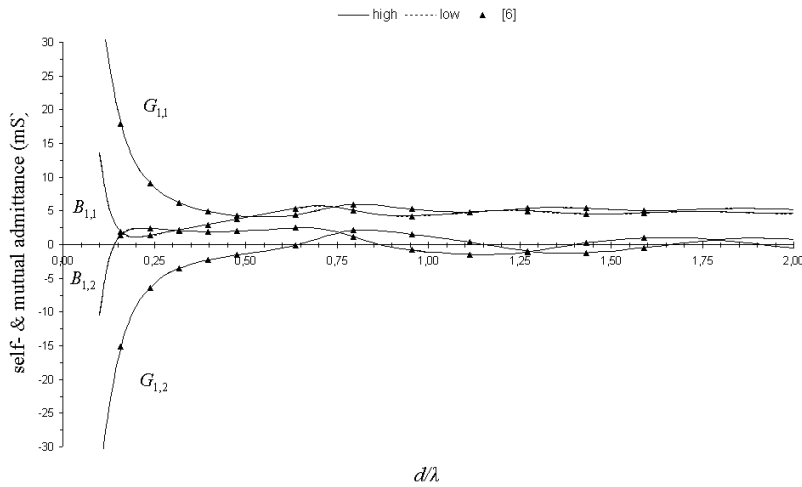


**Figure 4.** Plot of the self- and mutual admittances of two parallel identical loops as functions of  $d/\lambda$ , as derived by the RM scheme, for  $k_0b = 1$ ,  $\Omega = 2 \ln(2\pi b/a) = 10$  and  $c/a = 2.3$ . High and low discretization levels correspond to  $N = 75$  and  $N = 25$ , respectively.

version of the LU solver provided in [21], the number of operations required by the PM code is roughly approximated as

$$C_{\text{PM}} \approx \left( \sum_{p=1}^L 2N_p \right) (50G + 20) + \left[ \left( \sum_{p=1}^L 2N_p \right)^2 - \sum_{p=1}^L (2N_p)^2 \right] (50G + 7) \\ + \frac{2 \left( \sum_{p=1}^L 2N_p \right)^3 + 15 \left( \sum_{p=1}^L 2N_p \right)^2 + 13 \left( \sum_{p=1}^L 2N_p \right)}{3}. \quad (12)$$

As for the RM code, it is quite difficult to derive a closed-form expression for the number of operations required for filling the interaction matrix and the excitation vector using (10) and (11) on the basis of any threshold criterion. Nevertheless, it is quite easy to estimate an upper bound for the cost function of the RM code by assuming that (10) is utilized only for  $p \neq q$  and (11) is not used at all. This expression for the cost function is

$$C_{\text{RM}} \approx \left( \sum_{p=1}^L 2N_p \right) (100G^2 + 50G + 3) \\ + \left[ \left( \sum_{p=1}^L 2N_p \right)^2 - \sum_{p=1}^L (2N_p)^2 \right] (100G + 17) \\ + \frac{2 \left( \sum_{p=1}^L 2N_p \right)^3 + 15 \left( \sum_{p=1}^L 2N_p \right)^2 + 13 \left( \sum_{p=1}^L 2N_p \right)}{3}. \quad (13)$$

In the special case of identical elements (namely, when  $b_p = b$  and  $a_p = a$ ),  $N_1 = N_2 = \dots = N_L$  and the above formulas are reduced to

$$C_{\text{PM}} \approx L(50G + 20)(2N_{\text{PM}}) + L(L - 1)(50G + 7)(2N_{\text{PM}})^2 \\ + \frac{2L^3(2N_{\text{PM}})^3 + 15L^2(2N_{\text{PM}})^2 + 13L(2N_{\text{PM}})}{3}, \quad (14)$$

$$C_{\text{RM}} \approx L(100G^2 + 50G + 3)(2N_{\text{RM}}) + L(L - 1)(100G + 17)(2N_{\text{RM}})^2 \\ + \frac{2L^3(2N_{\text{RM}})^3 + 15L^2(2N_{\text{RM}})^2 + 13L(2N_{\text{RM}})}{3}. \quad (15)$$

As in [18], these expressions can be utilized in many ways; for example, one can set  $N_{\text{RM}} = \kappa N_{\text{PM}}$  (with  $N_{\text{PM}} \sim \pi b/a$ ) and proceed to

determine the range of  $\kappa$  for which the RM scheme should be preferred to the PM one. Alternatively, one can choose a fairly small  $\kappa$  (for example,  $\kappa = 0.25$ ) and proceed to obtain which  $N_{\text{PM}}$  (or  $\pi b/a$ ) satisfy the inequality  $C_{\text{PM}} - C_{\text{RM}} \geq 0$ . For this, the roots of the equation  $C_{\text{PM}} - C_{\text{RM}} = 0$  are obtained, which are expressed as

$$2N_{\pm} = \frac{-P_1 \pm \sqrt{P_1^2 - 4P_0P_2}}{2P_2}, \quad (16)$$

where  $P_0 = L[-100G^2\kappa - 50G(\kappa - 1) + (73 - 22\kappa)/3]$ ,  $P_1 = L(L - 1)(50G + 7 - 100G\kappa^2 - 17\kappa^2) + 5(1 - \kappa^2)L^2$  and  $P_2 = 2(1 - \kappa^3)L^3/3$ . For  $\kappa < 1$ ,  $P_2$  is always positive, but the signs of  $P_0$  and  $P_1$  depend on  $G$  and  $\kappa$ . It can be easily shown that  $P_0$  is negative when

$$G > \frac{1 - \kappa}{4\kappa} + \frac{\sqrt{75 + 142\kappa - 13\kappa^2}}{20\sqrt{3}\kappa}. \quad (17)$$

Within the interval of interest  $0.1 \leq \kappa < 1$ , (17) holds for  $G \geq 5$ ; under this latter condition, the roots given by (16) are real numbers with  $N_- < 0$  and  $N_+ > 0$ . Under these circumstances, the inequality  $C_{\text{PM}} - C_{\text{RM}} > 0$  is satisfied for  $N_{\text{PM}} > N_+$ . On the other hand, when  $P_0 > 0$  and  $P_1^2 > 4P_0P_2$ , the roots  $N_{\pm}$  and  $P_1$  have opposite signs; thus, when  $P_1 > 0$ , the roots  $N_{\pm}$  are both negative and the inequality  $C_{\text{PM}} - C_{\text{RM}} > 0$  is satisfied for all positive  $N_{\text{PM}}$ . Nevertheless, this latter case is of limited usefulness, as long as it occurs for quite small  $G$ , which cannot guarantee the accuracy of the computations. Finally, elementary investigation of the inequalities  $P_0 > 0$  and  $P_1 < 0$  has revealed that they cannot hold simultaneously for any meaningful combination of the parameters  $L$ ,  $G$  and  $\kappa$ .

Several tests have confirmed the findings of the last paragraph. As an indicative example, a coaxial array of four identical elements with  $\pi b/a \approx 110$  ( $b/\lambda = 0.1572$ ,  $a/\lambda = 0.004496$ ) and  $c/a = 2.3$  is examined. Measured execution times, normalized to that required by the PM code for  $N = 110$  (or a total number of  $2LN = 880$  unknowns), are depicted in Fig. 5 for  $G = 64$ . Even for this large  $G$ , as can be readily inferred from (14) and (15), the inequality  $C_{\text{RM}} < C_{\text{PM}}$  is satisfied for  $\kappa < 0.713$ . Obviously, this result agrees remarkably well with what should be expected from Fig. 5. As a second example, a Yagi array of loops is examined, which is taken from [19] and consists of a reflector with  $k_0b_1 = 1.05$ , a frill-driven exciter with  $k_0b_2 = 1.1$  and  $c_2/a = 2.3$ , as well as  $L - 2$  directors with  $k_0b_p = 0.9$  (where  $p = 3, 4, \dots, L$ ). The wire radius of all elements is selected so that  $\Omega_2 = 2 \ln(2\pi b_2/a) = 11$  (or, equivalently,  $a/\lambda = 0.004496$ ). As in [19], the reflector is situated at  $z_1 = -0.1\lambda$ , while the exciter

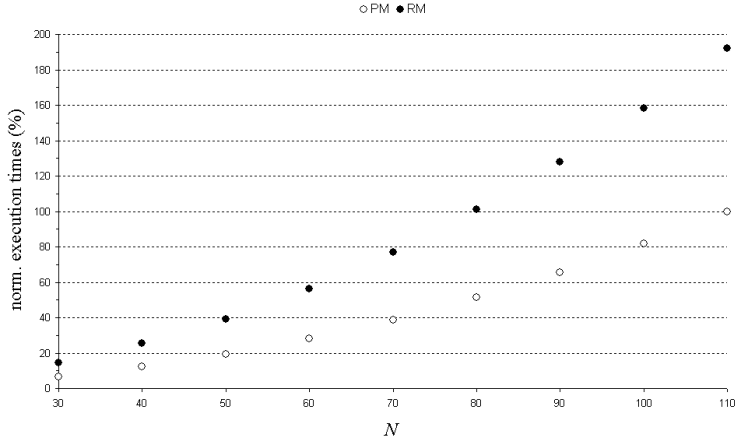


**Figure 5.** Normalized execution times for a four-element array of loops with  $\pi b/a \approx 110$  ( $b/\lambda = 0.1572$ ,  $a/\lambda = 0.004496$ ) and  $c/a = 2.3$ .

is at  $z_2 = 0$ . The directors are located at  $z_p = (p - 2)d$ , where  $d = 0.2\lambda$ . Results for the measured execution times, normalized to that required by the PM code for  $N_p$  close to  $\pi b_p/a$  (namely,  $N_1 = 117$ ,  $N_2 = 123$  and  $N_3 = \dots = N_L = 101$ ) are depicted in Fig. 6. In this example, the RM runs were performed with  $N_1 = 30$ ,  $N_2 = 31$  and  $N_3 = \dots = N_L = 26$ . Results for the computed input admittance are also provided in Table 1, together with the ones reported in [19]. As can be seen from Fig. 6 and Table 1, the savings in the execution times are greater than 85%, without significant accuracy loss (the differences in the computed conductance and susceptance were found to be smaller than 2%).

**Table 1.** Results for the input admittance of various Yagi arrays consisting of a reflector with  $k_0 b_1 = 1.05$ , a frill-driven exciter with  $k_0 b_2 = 1.1$  and  $c_2/a = 2.3$ , as well as  $L - 2$  directors with  $k_0 b_p = 0.9$  (where  $p = 3, 4, \dots, L$ ). The wire radius of all elements is  $a/\lambda = 0.004496$ , the reflector-exciter spacing is  $z_2 - z_1 = 0.1\lambda$  and the directors are spaced apart by  $d = 0.2\lambda$ .

$L$	Input Admittance (mS)		
	PM (117, 123, 101, ... 101)	RM (30, 31, 26, ... 26)	Results from [19]
4	$1.616 - j5.176$	$1.600 - j5.103$	$1.60 - j5.18$
6	$1.550 - j5.377$	$1.534 - j5.299$	$1.56 - j5.38$
8	$1.538 - j5.576$	$1.518 - j5.494$	$1.54 - j5.58$

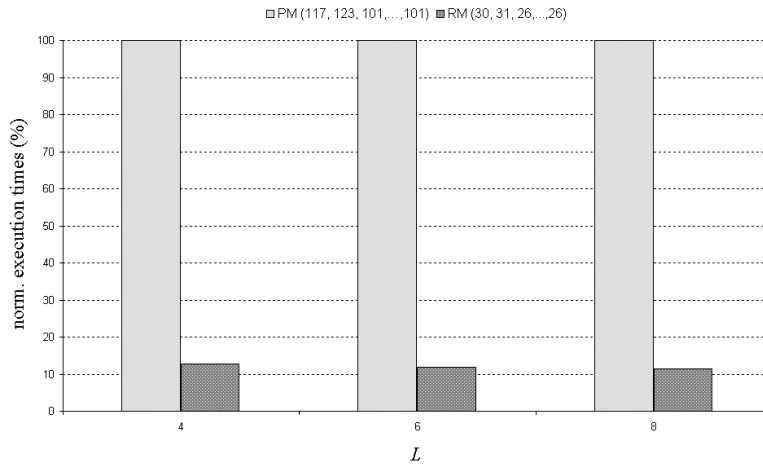


**Figure 6.** Normalized execution times for the arrays of Table 1.

## 5. SUMMARY AND CONCLUDING REMARKS

A direct sub-domain moment-method formulation was presented for the analysis of arrays of thin-wire loops. Curved piecewise sinusoids were assumed as basis functions, while both a simple collocation technique and Galerkin's method were applied for testing. Numerical results were presented for regular arrays to verify the developed codes and validate the results, but also to delve into the behavior of the solutions as the number of basis functions grows.

Cost functions were derived for the developed codes, in order to make complexity estimations and comparisons on a fair and meaningful basis. From the complexity analysis and the numerical results presented, general guidelines were extracted for the efficient implementation of the proposed schemes.

## ACKNOWLEDGMENT

The author wishes to thank Dr. G. Fikioris and Dr. H. T. Anastassiou for their suggestions and comments. This work was conducted as part of a post-doc research program supported by the State Scholarships Foundation of Greece.

## REFERENCES

1. Wu, T. T., "Theory of the thin circular loop antenna," *Journal of Mathematical Physics*, Vol. 3, No. 6, 1301–1304, 1962.
2. King, R. W. P., "The loop antenna for transmission and reception," *Antenna Theory*, R. E. Collin and F. J. Zucker (eds.), Ch. 11, McGraw-Hill, New York, 1969.
3. King, R. W. P. and C. W. Harrison, *Antennas and Waves: A Modern Approach*, Ch. 9, M.I.T. Press, Cambridge, MA, 1969.
4. Esselle, K. P. and S. S. Stuchly, "Resistively loaded loop as a pulse-receiving antenna," *IEEE Transactions on Antennas and Propagation*, Vol. 38, No. 7, 1123–1126, 1990.
5. Zhou, G. and G. S. Smith, "An accurate theoretical model for the thin-wire circular half-loop antenna," *IEEE Transactions on Antennas and Propagation*, Vol. 39, No. 8, 1167–1177, 1991.
6. Iizuka, K., R. W. P. King, and C. W. Harrison, "Self- and mutual admittances of two identical circular loop antennas in a conducting medium and in air," *IEEE Transactions on Antennas and Propagation*, Vol. 14, No. 4, 440–450, 1966.
7. Ito, S., N. Inagaki, and T. Sekiguchi, "An investigation of the array of circular-loop antennas," *IEEE Transactions on Antennas and Propagation*, Vol. 19, No. 4, 469–476, 1971.
8. Abul-Kassem, A. S. and D. C. Chang, "On two parallel loop antennas," *IEEE Transactions on Antennas and Propagation*, Vol. 28, No. 4, 491–496, 1980.
9. Huang, Y., A. Nehorai, and G. Friedman, "Mutual coupling of two collocated orthogonally oriented circular thin-wire loops," *IEEE Transactions on Antennas and Propagation*, Vol. 51, No. 6, 1307–1314, 2003.
10. Krishnan, S., L.-W. Li, and M.-S. Leong, "Comments on 'Mutual coupling of two collocated orthogonally oriented circular thin-wire loops'," *IEEE Transactions on Antennas and Propagation*, Vol. 52, No. 6, 1625–1626, 2004.
11. Harrington, R. F., *Field Computation by Moment Methods*, MacMillan, New York, 1968.
12. Champagne II, N. J., J. T. Williams, and D. R. Wilton, "The use of curved segments for numerically modeling thin wire antennas and scatterers," *IEEE Transactions on Antennas and Propagation*, Vol. 40, No. 6, 682–689, 1992.

13. Selçuk, A. and B. Saka, "A general method for the analysis of curved wire antennas," *Journal of Electromagnetic Waves and Applications*, Vol. 21, No. 2, 175–188, 2007.
14. Li, L.-W., C.-P. Lim and M.-S. Leong, "Method-of-moments analysis of electrically large circular-loop antennas: Nonuniform currents," *IEE Proceedings on Microwaves, Antennas and Propagation*, Vol. 146, No. 6, 416–420, 1999.
15. Krishnan, S., L.-W. Li, and M.-S. Leong, "Entire-domain MoM analysis of an array of arbitrarily oriented circular loop antennas: A general formulation," *IEEE Transactions on Antennas and Propagation*, Vol. 53, No. 9, 2961–2968, 2005.
16. Anastassiou, H. T., "Fast, simple and accurate computation of the currents on an arbitrarily large circular loop antenna," *IEEE Transactions on Antennas and Propagation*, Vol. 54, No. 3, 860–866, 2006.
17. Anastassiou, H. T., "An efficient algorithm for the input susceptance of an arbitrarily large, circular loop antenna," *Electronics Letters*, Vol. 42, No. 16, 897–898, 2006.
18. Papakanellos, P. J., "Alternative sub-domain moment methods for analyzing thin-wire circular loops," *Progress In Electromagnetics Research*, PIER 71, 1–18, 2007.
19. Shoamanesh, A. and L. Shafai, "Design data for coaxial Yagi array of circular loops," *IEEE Transactions on Antennas and Propagation*, Vol. 27, No. 5, 711–713, 1979.
20. Avdikos, G. K. and H. T. Anastassiou, "Computational cost estimations and comparisons for three methods of applied electromagnetics," *IEEE Antennas and Propagation Magazine*, Vol. 47, No. 1, 121–129, 2005.
21. Press, W. H., S. A. Teukolsky, W. T. Vetterling, and B. P. Flannery, *Numerical Recipes in C*, Cambridge University Press, New York, 1992.